Journal of Neuropathology and Experimental Neurology

Vol. 59, No. 6
June, 2000
pp. 513–524

A Qualitative and Quantitative Study of Grumose Degeneration in Progressive Supranuclear Palsy

KEISUKE ISHIZAWA, MD, WEN-LANG LIN, PHD, PAUL TISEO, MS, WILLIAM G. HONER, MD, PETER DAVIES, PHD, AND DENNIS W. DICKSON, MD

Abstract. Grumose degeneration (GD) of the dentate nucleus is a common feature in progressive supranuclear palsy (PSP), but its pathogenesis has not been well studied, and its clinical significance remains unknown. This report describes a quantitative study of GD in 9 cases of PSP using image analysis with single- and double-immunolabeling, as well as histochemical stains for myelin and axons. GD was associated with demyelination, axonal loss, glial tau pathology, and microgliosis in regions juxtaposed to the dentate nucleus (DN). Specifically, demyelination and microgliosis were prominent in the superior cerebellar peduncle (SCP), dentate hilus, and cerebellar hemispheric white matter. Tau pathology and microgliosis were less prominent in the DN itself. The degree of myelin loss correlated with the tau burden in the SCP. GAP-43, which is a phosphoprotein known to be involved in axonal growth and sprouting, was decreased in the DN of PSP, and the degree of GAP-43 loss correlated with severity of GD. These results suggest that GD may be related to progressive pathology in the dentatorubrothalamic tract as well as the cerebellar hemispheric white matter, and that GD may be a consequence of concurrent degeneration in both output from and input to the DN. The results further suggest a possible role for oligodendroglial and myelin pathology in the pathogenesis of PSP.

Key Words: Dentate nucleus; Grumose degeneration; Microglia; Oligodendroglia; Progressive supranuclear palsy; Tau.

INTRODUCTION

Grumose degeneration (GD) in the dentate nucleus was first described in progressive supranuclear palsy (PSP) (1). Subsequently, GD has been reported in various pathologic conditions such as CAG triplet repeat diseases (2, 3), perinatal hypoxic ischemic encephalopathy (4), and other disorders (2, 4, 5). Histologically, GD is characterized by eosinophilic, granular, and amorphous material around dentate neurons and their processes (2, 6, 7). There have been few systematic studies of this peculiar form of dentate nucleus pathology. As a result, little is known of the pathogenesis and clinical significance of GD. In order to understand its pathogenesis, it is important to consider the normal connectivity of the dentate nucleus. Axons of the cerebellar dentate neurons project via the superior cerebellar peduncle and red nucleus to the contralateral ventrolateral nucleus of the thalamus in the dentatorubrothalamic tract (8). It is common to find pathology in the dentatorubrothalamic tract in PSP (9), and these changes may contribute to some of the clinical features of PSP, such as frequent falls and postural instability (10). The red nucleus and ventrolateral nucleus of the thalamus are also targets of neuronal and glial tau pathology in PSP (9, 11). Furthermore, demyelination is often striking in the superior cerebellar peduncle and dentate hilus in PSP (1, 6, 12–14). In preliminary studies, we noted marked microglial activation in the dentatorubrothalamic pathway in PSP that suggested the possibility that pathology in the outflow pathway of the dentate nucleus might contribute to GD. The purpose of the present study was to systematically address this question by examining the dentate nucleus and its outflow pathway. Although GD is clearly not specific to PSP, PSP may well be the most common condition associated with GD. Therefore, a detailed study of GD in PSP may provide insights into the pathogenesis of GD in other disorders.

Morphologic studies of GD have documented degenerating synaptic terminals of presumed Purkinje cell origin surrounding soma and dendrites of dentate neurons (2, 7). These observations lead to the hypothesis that GD was due to Purkinje cell axonal pathology ''upstream'' of the dentate nucleus. GD was considered to be due to sprouting or regeneration of presynaptic terminals (7, 15, 16). If this is correct, we speculated that immunostaining for GAP-43, which is a phosphoprotein found in axonal growth cones and presynaptic nerve terminals whose expression is associated with neuronal outgrowth and new terminal formation (17–19), might prove to be a useful way to verify this hypothesis.

MATERIALS AND METHODS

Nine cases of PSP and 4 normal controls were studied. Table 1 lists their clinical features. A right or left cerebral hemisphere removed at autopsy was fixed in 10% buffered formalin and sections were processed for paraffin embedding. Consecutive 5-μm-thick horizontal sections of the cerebellum at the level of

From the Department of Pathology (KI, W-LL, PT, DWD), Mayo Clinic Jacksonville, Jacksonville, Florida; Department of Psychiatry (WGH), University of British Columbia, Vancouver, British Columbia; Departments of Pathology and Neuroscience (PD), Albert Einstein College of Medicine, Bronx, New York.

Supported by the Eloise H. Troxel Memorial Grant of the Society for Progressive Supranuclear Palsy, NIH AG03949-13, NIH AG14449-2, NIH AG17216-1, and the Mayo Foundation. WGH receives support from a Scientist Award from the Medical Research Council of Canada.

Correspondence to: Dennis W. Dickson, MD, Department of Pathology, Mayo Clinic Jacksonville, 4500 San Pablo Road, Jacksonville, FL 32224.

TABLE 1
Clinical Features of the Cases Studied

Case No.	Age	Sex	Diagnosis	GD grade	PMI (hours)
1	68	M	PSP	I	5.0
2	71	M	PSP	I	4.0
3	74	F	PSP	I	5.0
4	70	F	PSP	II	NA
5	78	M	PSP	II	5.0
6	82	F	PSP	II	7.0
7	65	M	PSP	III	5.0
8	70	F	PSP	III	NA
9	NA	M	PSP	III	NA
10	94	M	NC		NA
11	81	M	NC		NA
12	59	NA	NC		NA
13	86	F	NC		24.0

Abbreviations: PSP, progressive supranuclear palsy; GD, grumose degeneration; PMI, postmortem interval; NC, normal control; NA, not available.

the dentate nucleus, the pons containing the locus ceruleus at the level of the superior cerebellar peduncle, the midbrain at the level of the red nucleus, and coronal sections through the mammillothalamic tract containing the ventrolateral nucleus of the thalamus served for this study.

Double-labeling Immunohistochemistry

The deparaffinized and rehydrated sections of the cerebellum were incubated in 0.01 M phosphate buffered saline (PBS; pH 7.4) containing 0.3% hydrogen peroxide for 30 minutes, washed in PBS and then microwaved in distilled water at high power setting for 10 minutes. An anti-synaptophysin antibody, which is a good marker for GD (4), was used to immunostain GD in this study. The sections were treated with 5% normal goat serum for 10 minutes and incubated overnight in a cocktail of 2 different primary antibodies: 1) monoclonal anti-synaptophysin (EP10; 1:5; IgG1) (20) and anti-tau antibodies (Alz-50; 1:5; IgM) (21); 2) EP10 and a monoclonal anti-phosphorylated neurofilament antibody (NP16; 1:5; IgM) (22); 3) EP10 and a monoclonal anti-class II major histocompatibility complex (MHC II) antibody for activated microglia (LN-3; 1:5; IgG2b; ICN Biomedical, Inc.; Aurora, OH) (23); 4) EP10 and a polyclonal anti-glial fibrillary acid protein antibody (GFAP; 1:1,000; BioGenex; San Ramon, CA) for astrocytes. When EP10 failed to yield a satisfactory staining, a monoclonal anti-synaptobrevin antibody (SP11; 1:5; IgG1) (24) was substituted. EP10 and SP11 showed almost complete overlap of stained structures and were essentially interchangeable, but in some cases SP11 gave more robust staining than EP10. The sections were treated with a cocktail of biotin-conjugated and alkaline phosphatase (AP)-conjugated goat secondary antibodies (1:100; Southern Biotechnology Assoc.; Birmingham, AL) for 2 hours and then incubated in a cocktail of avidin/biotinylated enzyme complex reagent (1:200; Vectastain ABC kit; Vector Lab.; Burlingame, CA) and the same AP-conjugated antibody for 2 hours. The choice of the 2 secondary antibodies was dependent on the species and isoform of the primary antibodies. This procedure allowed detection of an epitope of 1 of the 2 antibodies with an avidin-biotin amplification method. After being washed in PBS, the sections were treated with diaminobenzidine (DAB) for a few minutes followed by 5-bromo-4-chloro-3-indolyl phosphate/nitro blue tetrazolium (BCIP/NBT) for 10 to 20 minutes. The sections were dehydrated with increasing concentrations of ethanol followed by xylene, then mounted and coverslipped.

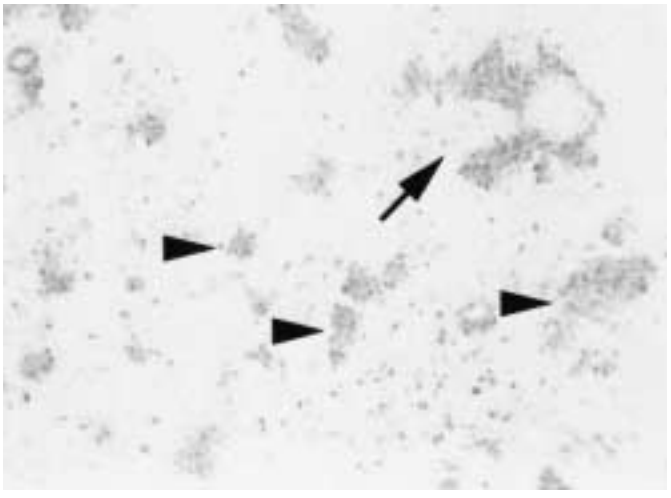

Fig. 1. Immunostaining with SP11 in the dentate nucleus of PSP displays GD, (224×). Morphological criteria for GD to be counted are shown: variable-sized immunoreactive granules aggregated around neuronal soma or processes whose morphological details are obscured (arrow); and clusters of variable-sized immunoreactive granules or immunoreactive spherical structures without visible neuronal soma or processes (arrowheads). Both types of GD were included in the counting.

Myelin and Axon Analysis

The sections of the cerebellum, pons, midbrain, and thalamus were immunostained with LN-3 using an immunoperoxidase method (ABC technique; Vectastain ABC kit; Vector Lab.) or double-immunostained with LN-3 and a monoclonal anti-tau (PHF-1; 1:100; IgG1) (25) antibody as previously described. After the treatment with DAB and BCIP/NBT, the sections were counterstained with Luxol fast blue (LFB) for myelin. LFB has been effectively used in other studies of myelin changes in human neuropathology, for example in developmental studies of brain myelination (26). The immunostained sections were microwaved in 0.1% LFB solution for 80 seconds. After the incubation in an oven at 65°C for 30 minutes, the sections were rinsed in 95% alcohol and immersed in 0.05% lithium carbonate. The sections were dehydrated, mounted, and coverslipped. Some of the immunostained sections were also counterstained with both LFB and Bodian silver method for axon.

Quantitative Analysis

For quantification of GD, the sections of the cerebellum were immunostained with EP10 or SP11 with DAB as the chromogen. Sections used for image analysis were not counterstained. Morphological criteria for GD for counting purposes were as follows and illustrated in Figure 1: A cluster of variable-sized immunoreactive granules that aggregated around neuronal soma

or processes whose morphological details were obscured by the granular structures; or a cluster of variable-sized immunoreactive granules or an immunoreactive spherical structures without visible neuronal soma or processes. Both types of granules were included in the counts since previous studies have emphasized that GD forms along dendritic arbors without a clearly identified cell body as ''coarsely granular, slightly eosinophilic, mostly anuclear cellular bodies of degenerated nerve cells'' (1, 7). The method for counting GD is as follows: an area with the most GD was identified at low magnification, and this area was scanned for GD in adjacent 40 fields at high magnification (400×) moving along the dentate ribbon; the number was expressed as an average of 10 fields. For purposes of correlation analysis, the 9 PSP cases were divided into 3 grades of GD: grade I (≤10 GD/400×; N = 3), grade II (>10 GD/400×, but <50 GD/400×; N = 3), and grade III (≥50 GD/400×; N = 3) (Table 1).

For correlation analysis with GD grading, the adjacent sections of the interested areas were stained with LFB for myelin and Bodian's silver stain for axons and immunostained with LN-3 or PHF-1. In addition, adjacent sections of the cerebellum were immunostained with GAP-43 and a monoclonal anti-phosphorylated neurofilament antibody (SMI31; 1:1,000; IgG1) (27) for Purkinje cell axonal torpedoes. To increase uniformity of histochemical analyses, all cases were stained for LFB and Bodian's stain as a batch with identical solutions and incubation times. The procedures for immunostaining used the ABC technique.

After identifying a representative field with high density of immunolabeling with LN-3, PHF-1 or GAP-43 at low magnification, the area was scanned at high magnification (400×), and a total of 4 images (totaling 0.1 mm^2) were captured from each area using image analysis software (Intellicam 2.0; Matrox Electronic Systems, Ltd.; Quebec, Canada) with a light microscope (BH-2-RFCA; Olympus; Melville, NY) equipped with a color video camera (Javelin; Javelin Electronics; Los Angeles, CA). The analyzed areas included ventrolateral nucleus of the thalamus (VL), red nucleus (RN), superior cerebellar peduncle (SCP), dentate hilus (DH), dentate nucleus (DN), and cerebellar hemispheric white matter (cerebellar WM). For LFB- or Bodian-stained sections, representative fields with the greatest loss of myelin or axon staining were identified and these fields served as targets for image capture from the RN, SCP, and DH.

The captured images were processed with image analysis software (SigmaScan Pro 3; Jandel Scientific; San Rafael, CA), converted to gray-scale images, and labeling was defined by its intensity. The whole area occupied by the labeling was measured in pixels, and a ratio of the immunoreactive pixels to the total pixels of the whole field (0.025 mm^2/field) was calculated to yield an estimate of lesion burden. Labeling of red blood cells was edited before analysis of LFB-stained sections. Similarly, labeling of nuclei and blood vessels was edited before analysis of Bodian silver-stained sections.

The number of Purkinje axonal torpedoes was counted using neurofilament (SMI-31)-immunostained sections. The cerebellar cortex was scanned at magnification (100×) until one or more torpedoes were identified. The field was selected to maximize the density of torpedoes. The counting was performed in 30 intermittent fields and was expressed as an average count per field. The data were analyzed with a computer software system (Stat-View 4.0; Abacus Concept; Berkeley, CA).

RESULTS

Qualitative Analysis of GD

Tau-positive neurofibrillary tangles and neuropil threads, which were absent in controls, were relatively sparse in the DN of PSP. The cases with the most marked GD had less tau pathology than PSP cases with little or no GD. Most of GD-positive neurons did not have tau immunoreactivity (Fig. 2A). Likewise, only a small proportion of tau-immunoreactive neurons had GD (Fig. 2B). The same was true for neurofilament immunostaining; that is, most GD-positive neurons were neurofilament-negative (Fig. 3A) and most neurofilament-positive neurons were GD-negative (Fig. 3B). Some of the granules in GD were neurofilament-positive but tau-negative. Microglia were increased both in number and area in the DN; however, aggregated or ameboid microglia were more numerous in the white matter of the dentate hilus than in the nucleus itself (Fig. 4A). Moreover, microglia were not necessarily associated with neurons undergoing GD (Fig. 4B). Astrocytic fibrillary gliosis was prominent in most cases, but again not spatially associated with neurons displaying GD. Astrocytic processes were diffuse throughout the DN (Fig. 5). GAP-43 immunoreactivity was recognized as punctate granules in the neuropil or around neuronal soma. While GAP-43 immunoreactivity was aligned along neuronal processes in controls (Fig. 6A), most of the granules in GD were devoid of GAP-43 immunoreactivity (Fig. 6B). Furthermore, compared with controls, GAP-43 immunoreactivity was clearly decreased in PSP, and the most striking decrease was in cases with the most marked GD (Fig. 6).

In all the regions of PSP studied, microglia were remarkably increased both in number and area (Figs. 7, 8). Loss or destruction of myelin was conspicuous in the dentatorubrothalamic tract, and axons were often shrunken or left naked, especially in the DH and SCP (Figs. 7, 8). Phagocytosis of myelin by microglia, characterized by myelin debris within the cytoplasm of MHC II-immunopositive microglia, was a common feature, especially in the DH and SCP (Figs. 7, 8D, F). Tau-positive lesions were numerous in the VL and RN (Fig. 8B, D). Most of the tau-positive glia in white matter were consistent with coiled bodies, and there were also many tau-positive cell processes aligned parallel with fiber tracts. Microglia and tau-positive lesions were not clearly juxtaposed or colocalized in the regions studied (Figs. 7, 8).

Quantitative Analysis

Microglial and tau burden were defined by the proportion of area occupied by LN-3 and PHF-1 immunoreactivity; myelin and axon areas by the proportion of area occupied by LFB and Bodian silver labeling; and

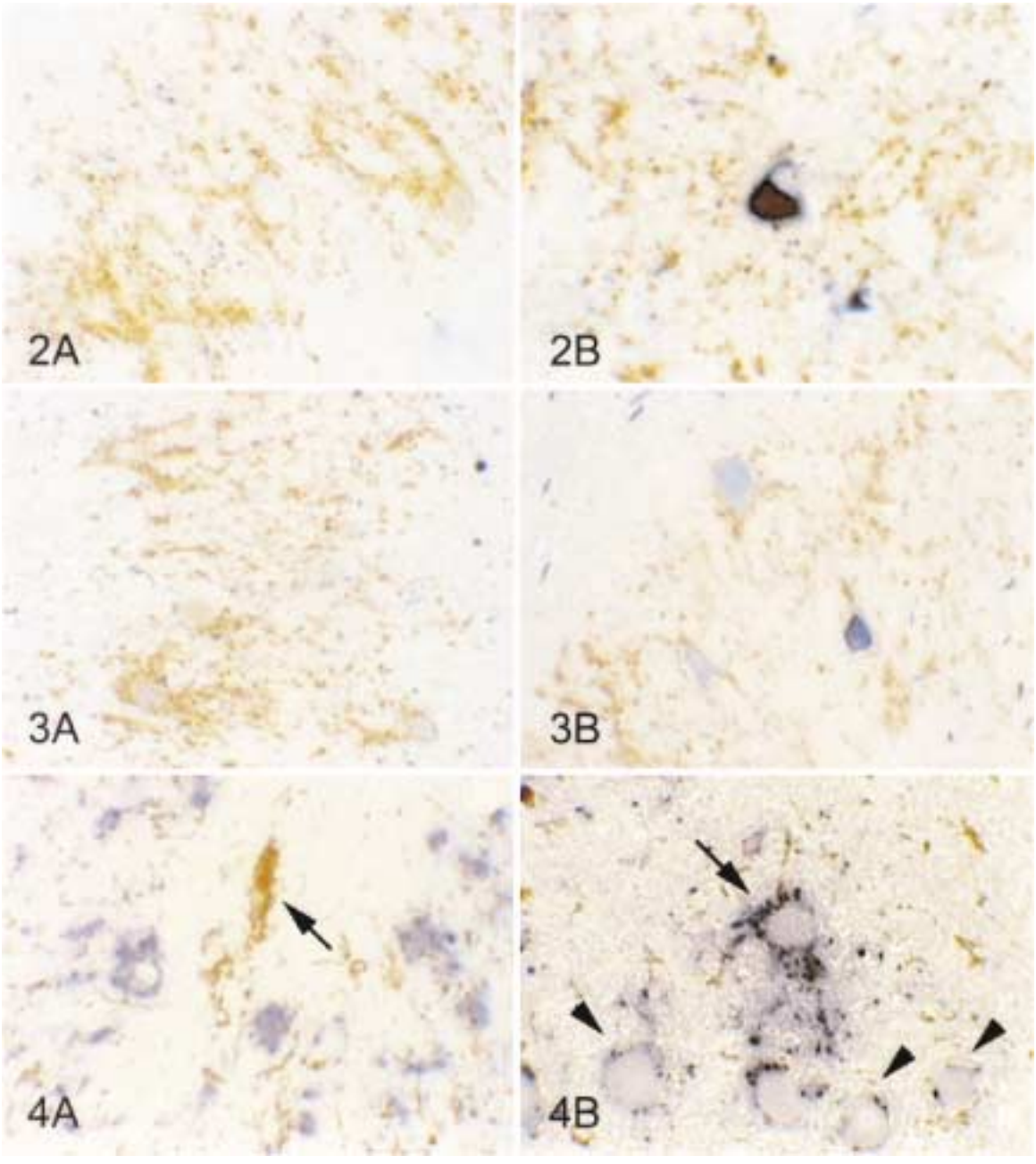

Fig. 2. Double-immunostaining with EP10 (brown) and Alz-50 (purple) in the dentate nucleus of PSP, (215×). A: Most of GD-positive neurons did not have Alz-50 immunoreactivity. B: Most of Alz-50-immunoreactive neurons did not have GD.

Fig. 3. Double-immunostaining with EP10 (brown) and NP16 (purple) in the dentate nucleus of PSP, (215×). A: Most GD-positive neurons were NP16-negative. B: Most NP16-positive neurons were GD-negative.

Fig. 4. Double-immunostaining with EP10 (purple) and LN-3 (brown) in the dentate nucleus of PSP, (215×). Microglia were increased both in number and area in the DN. A: Aggregated or ameboid microglia were more common in the dentate hilus than DN (arrow). B: Microglia showed no obvious spatial relationship to neurons with GD. The relationship of microglia to GD-positive neurons (arrow) and normal-looking neurons (arrowheads) is essentially the same.

GAP-43-positive area as the proportion of area occupied by GAP-43 immunoreactivity.

In all the regions studied, microglial burden was significantly and diffusely increased in PSP compared with controls (Table 2). The greatest relative increase was noted in the SCP. In PSP, myelin was significantly decreased in the cerebellar outflow pathway, that is, the DH, SCP, and RN (Table 2). In addition, the axonal area on Bodian stains was significantly decreased in the RN (Table 2). GAP-43 was significantly decreased in the

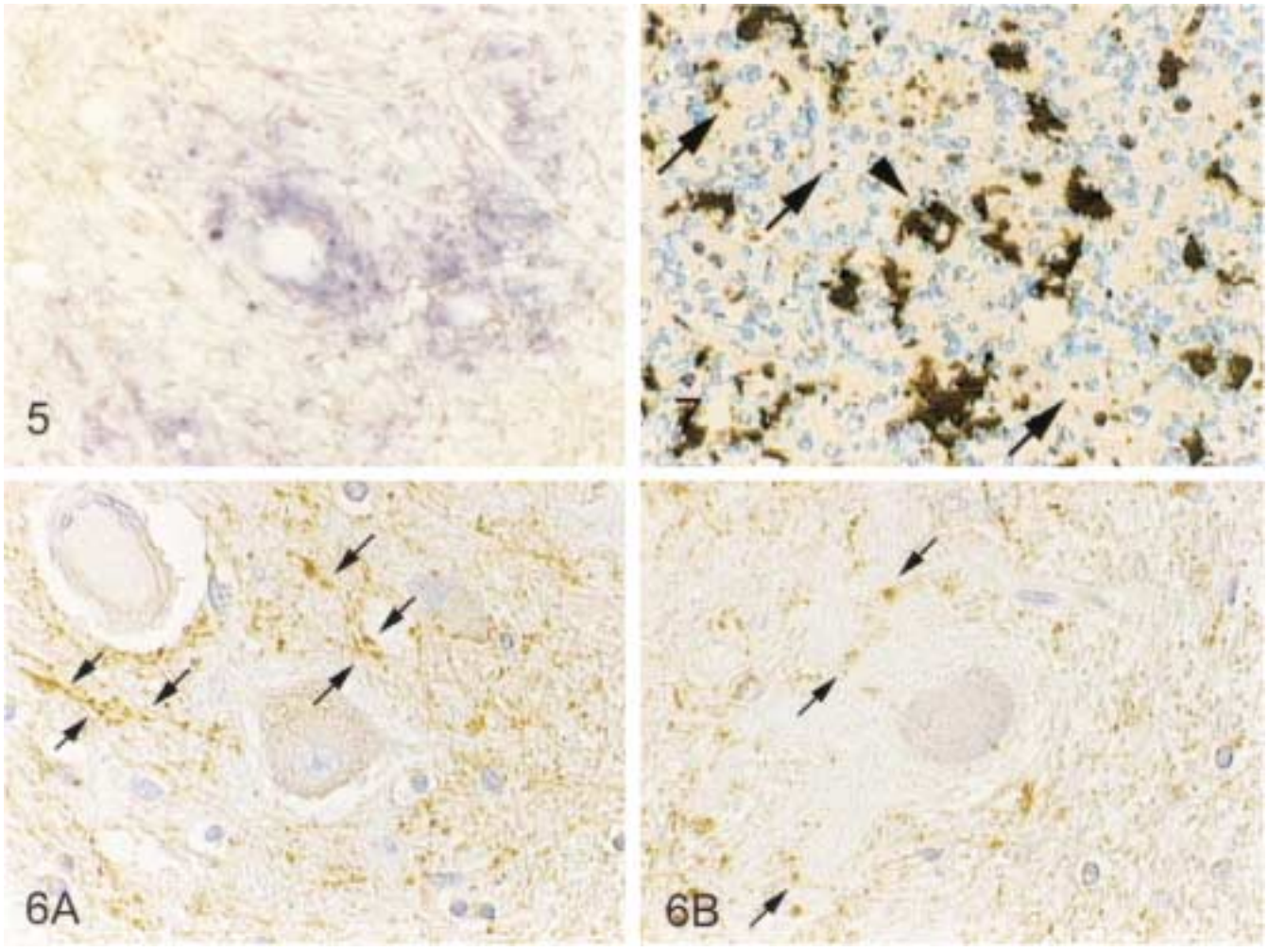

Fig. 5. Double-immunostaining with SP11 (purple) and GFAP (brown) in the dentate nucleus of PSP, (215×). Many GFAP-positive cell processes were diffusely distributed throughout the DN and not clearly increased in the vicinity of GD.

Fig. 6. Immunostaining with GAP-43 counterstained with hematoxylin in the dentate nucleus of controls (A) and PSP (B), (486×). GAP-43 immunoreactivity was recognized as punctate granules in the neuropil or around neuronal soma. A: Note an organized alignment of GAP-43 immunoreactivity along neuronal processes in controls (arrows). B: In contrast, most of the granules in GD are devoid of GAP-43 immunoreactivity, which, if any, seem to be dispersed to the periphery of GD (arrows). Furthermore, GAP-43 immunoreactivity in the DN was clearly decreased compared with controls.

Fig. 7. Immunostaining with LN-3 (dark brown) counterstained with LFB (blue) and Bodian's silver stain (gray) in the superior cerebellar peduncle of PSP, (430×). Microglia are increased both in number and volume in affected white matter tracts. Loss or destruction of myelin is conspicuous, and axons are often shrunken or left naked (arrows). Phagocytosis of myelin by microglia, where myelin debris is encompassed by cytoplasm of microglia, was a common finding (arrowhead).

DN of PSP compared with controls (Table 2). In PSP, tau burden was greatest in the VL and RN, but relatively sparse in the other regions included in the present study (average ± standard deviation (%); VL: 8.8 ± 3.9, RN: 7.5 ± 3.3, SCP: 0.7 ± 0.5, DH: 0.8 ± 0.5, DN: 2.7 ± 1.2, and cerebellar WM: 1.8 ± 1.3).

Pathology ''Downstream'' of the DN

For the purposes of description and discussion, the term ''downstream'' is used to refer to the various anatomic components of the dentatorubrothalamic pathway, including fiber tracts and gray matter areas. For example, both the SCP and the red nucleus are downstream of the DN. Similarly, ''upstream'' is used for anatomic structures in both gray and white matter that are related to projections to the DN. For example, Purkinje cells, their axons, and the cerebellar white matter are upstream of the DN.

Severity of GD correlated with microglial burden in the DH, but not with microglial burden in the DN or downstream regions (Table 3). Surprisingly, GD was inversely correlated with tau burden in both the DH and DN (Table 3). The correlation analysis between microglial burden and tau burden showed that microglial burden

TABLE 2
Microglial Burden, Myelin and Axonal Areas and GAP-43-immunoreactivity in PSP and Normal Controls

Neuroanatomic region		VL	RN	SCP	DH	DN	Cbl WM
Microglial burden (%)	PSP	5.4 ± 2.6**	5.8 ± 2.1**	5.7 ± 2.9**	4.6 ± 2.5**	4.0 ± 2.0*	5.0 ± 3.1*
	Controls	1.5 ± 1.1	2.5 ± 1.1	0.9 ± 0.4	2.3 ± 1.9	2.8 ± 1.3	3.4 ± 1.4
Myelin (%)	PSP		10.1 ± 4.3**	24.2 ± 10.0*	12.5 ± 5.8**		
	Controls		18.6 ± 3.9	30.0 ± 4.6	19.5 ± 4.0		
Axon (%)	PSP		6.7 ± 2.7**	9.2 ± 4.4			
	Controls		14.7 ± 4.1	9.1 ± 2.5			
GAP-43 (%)	PSP					1.7 ± 0.9**	
	Controls					3.2 ± 1.6	

Average ± Standard deviation (%); Welch's unpaired-t-test: * $p < 0.05$; ** $p < 0.01$. Abbreviations: PSP, progressive supranuclear palsy; VL, ventrolateral nucleus of the thalamus; RN, red nucleus; SCP, superior cerebellar peduncle; DH, dentate hilus; DN, dentate nucleus; Cbl WM, cerebellar hemispheric white matter.

TABLE 3
Correlations between GD Severity and Microglial and Tau Burdens

Neuro-anatomic region	Microglial burden						Tau burden					
	VL	RN	SCP	DH	DN	Cbl WM	VL	RN	SCP	DH	DN	Cbl WM
GD severity	n.s.	n.s.	n.s.	0.36*	n.s.	0.43*	n.s.	n.s.	n.s.	−0.38*	−0.48**	0.35*

Spearman rank order correlation coefficients: n.s., not significant; * $p < 0.05$; ** $p < 0.01$. Abbreviations: VL, ventrolateral nucleus of the thalamus; RN, red nucleus; SCP, superior cerebellar peduncle; DH, dentate hilus; DN, dentate nucleus; Cbl WM, cerebellar hemispheric white matter.

TABLE 4
Correlations between Microglial and Tau Burdens

Neuro-anatomic region	Microglial burden					
	VL	RN	SCP	DH	DN	Cbl WM
Tau burden	0.72*	n.s.	n.s.	n.s.	n.s.	n.s.

Spearman rank order correlation coefficients: n.s., not significant; * $p < 0.05$. Abbreviations: VL, ventrolateral nucleus of the thalamus; RN, red nucleus; SCP, superior cerebellar peduncle; DH, dentate hilus; DN, dentate nucleus; Cbl WM, cerebellar white matter.

TABLE 5
Correlations between GD Severity and Myelin and Axonal Areas

Neuro-anatomic region	Myelin area			Axonal area	
	RN	SCP	DH	RN	SCP
GD severity	n.s.	−0.61**	−0.42*	n.s.	−0.38*

Spearman rank order correlation coefficients: n.s., not significant; * $p < 0.05$; ** $p < 0.01$. Abbreviations: RN, red nucleus; SCP, superior cerebellar peduncle; DH, dentate hilus.

was highly correlated with tau burden in the VL, but not in other regions (Table 4). Correlation analysis of GD with myelin and axon loss in the cerebellar outflow pathway demonstrated that myelin and axon area were inversely correlated with GD severity in the DH and SCP (Table 5). Correlation of microglial burden with myelin and axon areas, and of tau burden with myelin and axon areas were also analyzed. Tau burden was highly correlated with myelin loss in the SCP and RN, but not in the DH (Table 6). In contrast, microglial burden was not correlated with myelin loss in any of the 3 regions. Axon area was not correlated either with microglial burden or tau burden (Table 6).

Pathology "Upstream" of the DN

Severity of GD was significantly correlated with microglial burden and tau burden in the cerebellar WM (Table 3). Microglial burden was not correlated with tau burden in the cerebellar WM (Table 4). The degree of GAP-43 loss, but not the number of Purkinje cell axonal torpedoes, was significantly correlated with the severity of GD (Table 7). Moreover, the degree of GAP-43 loss was significantly correlated with microglial burden in the cerebellar WM (Table 8).

DISCUSSION

The results of the present study suggest that GD in PSP is associated with pathology both downstream and

upstream of the DN. In regard to downstream pathology, GD was associated with myelinated fiber loss, tau pathology, and microgliosis in the dentatorubrothalamic tract. In addition, pathology in distal portions of Purkinje cell axons and cerebellar WM constituted upstream pathology that correlated with GD in the DN. In contrast, intrinsic pathology of the DN was not clearly associated with GD. Neither DN neuronal pathology, as measured by aberrant tau and neurofilament immunoreactivity, nor reactive glial changes in the DN, as measured by microglial and astrocyte burden, showed any clear association with GD. Therefore, it is reasonable to suggest that pathology downstream and upstream, rather than in the DN itself, may contribute to GD. Based upon the above findings, although a direct correlation with GD is not proved, it is also reasonable to suggest that severe tau pathology in the VL and RN may contribute to GD.

Downstream Pathology

Our data show that pathology downstream of the DN is associated with GD. That neuronal pathology can occur in neuronal cell bodies in response to injury to the axon is analogous to chromatolysis, where axonal damage leads to retrograde alterations of neuronal perikarya (28). Although chromatolysis is best characterized in neurons whose axons lie within the peripheral nervous system (28), it can occur in the central nervous system (28–31). Dentate neurons with features resembling central chromatolysis have been described in previous studies of GD (2, 7). One might argue with the comparison of GD to chromatolysis, since axonal damage that is sufficient to produce chromatolysis is almost always an abrupt insult rather than a gradual neurodegenerative process as in PSP. There are other notable differences between experimental chromatolysis and GD. For example, perineuronal microgliosis is a consistent finding in chromatolysis, but it is not found in GD. GD is also different from chromatolysis in that there is also evidence of pathology upstream of the DN.

Given the pathology in the target zone of the dentatorubrothalamic tract, the findings may be closer to those found in retrograde transsynaptic degeneration, which has been studied experimentally and in human diseases. Experimental damage in the VL induces retrograde degeneration of the contralateral dentate nucleus (32), and cases of severe unilateral destruction of the thalamus, usually due to stroke, are natural models of retrograde transsynaptic degeneration in the dentatorubrothalamic tract (32, 33). An interesting PSP case has been reported with asymmetric, right-sided dominant lesions in the thalamus with left-sided dominant lesions in the dentate nucleus (34). Taken together with these reports, our data support the hypothesis that degeneration within the dentatorubrothalamic tract may contribute to GD in the DN. In support of this hypothesis, we found decreased myelin- and axon-labeling in the dentatorubrothalamic tract and positive correlations between severity of GD and myelin and axonal loss in these areas.

Axonal damage in demyelinating neurological disorders has increasingly been recognized (35–37). Myelin provides a trophic factor for axonal growth and maintenance, and its loss can result in axonal degeneration (37–39). For example, myelin-associated glycoprotein (MAG) has been shown to act as a modulator for maturation and viability of myelinated axons (40, 41). Conduction failure in some demyelinating disorders may be due to axonal injury. We have noted severe axonal pathology downstream of the DN. It is unclear whether this is due to intrinsic neurodegeneration or if it may be due to oligodendroglial pathology and myelin loss in these areas. The hypothesis that axonal damage may be secondary to oligodendroglial and myelin pathology downstream of the DN, which leads to GD in the DN, is worthy of further study, especially in disorders other than PSP in which GD has been described (2, 4, 5).

TABLE 6
Correlation between Microglial and Tau Burdens and Myelin and Axonal Areas

Neuroanatomic region	Myelin area			Axonal area	
	RN	SCP	DH	RN	SCP
Microglial burden	n.s.	n.s.	n.s.	n.s.	n.s.
Tau burden	−0.786*	−0.810*	n.s.	n.s.	n.s.

Spearman's rank order correlation coefficients: n.s., not significant; * $p < 0.05$. Abbreviations: RN, red nucleus; SCP, superior cerebellar peduncle; DH, dentate hilus.

TABLE 7
Correlation between GD Severity and Dentate GAP-43-immunoreactivity and Purkinje Cell Axonal Torpedoes

	GAP-43	Torpedoes
GD severity	−0.550**	n.s.

Spearman rank order correlation coefficients: n.s., not significant; ** $p < 0.01$.

TABLE 8
Correlations between Dentate GAP-43 Immunoreactivity and Microglial and Tau Burdens in the Cerebellar White Matter

	GAP-43
Microglial burden	−0.874*
Tau burden	n.s.

Spearman rank order correlation coefficients: n.s., not significant; * $p < 0.05$.

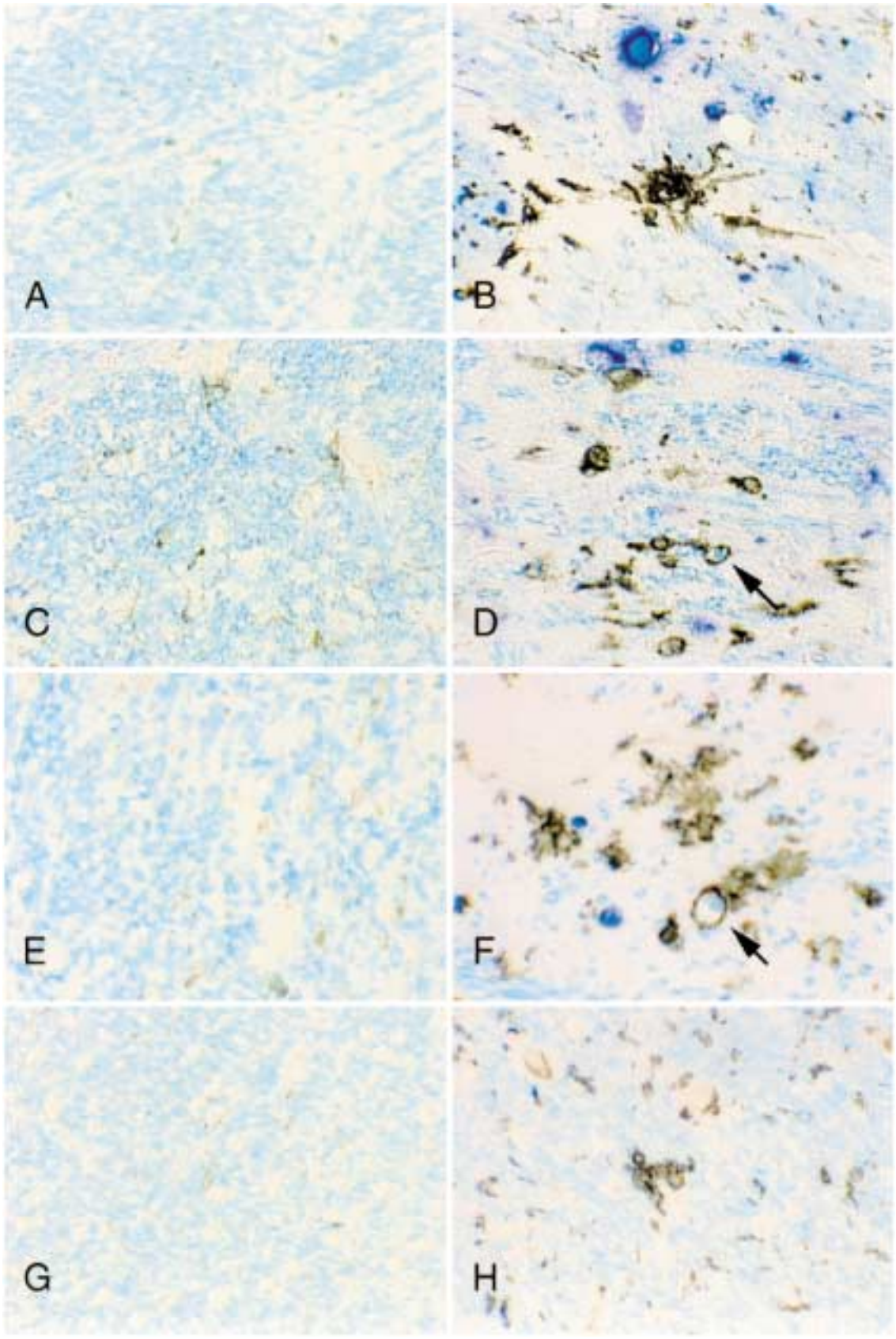

We have demonstrated that myelin loss was associated with tau burden in the SCP. Tau-positive lesions in the SCP are mostly in coiled bodies (42), which have been shown to be filamentous tau inclusions in oligodendrocytes. It is intriguing to speculate that oligodendrocyte tauopathy may contribute to myelin degeneration in PSP. To date there has been no direct demonstration that tau pathology in oligodendrocytes leads to impaired ability of oligodendrocytes to maintain myelin sheaths, but these observations bring to mind an analogous situation in multiple system atrophy (MSA). In MSA, glial cytoplasmic inclusions (GCI) in oligodendrocytes are a prominent histopathologic feature (43), and they are associated with widespread myelin pathology (44). A few electrophysiological studies in PSP have suggested the white matter involvement may have features consistent with demyelination (45, 46). In PSP and other neurodegenerative disorders, increased attention has been focused on glial inclusions or tau-positive thread-like structures (42, 43, 47, 48). Given the evidence of oligodendrocyte pathology in these disorders, it is surprising that to our knowledge there has been no previous study focusing on myelin pathology in PSP. Moreover, the influence of tau-positive inclusions on myelin integrity needs to be specifically addressed in future studies. Not all myelin loss was correlated with tau pathology in this study, which suggests that some myelin loss may be due to indirect injury. In particular, myelin loss in the DH was not accompanied by coiled bodies in the DH.

One might speculate that tau-positive oligodendroglial lesions might contribute to axonal pathology in the dentatorubrothalamic tract in PSP. It has been shown that oligodendrocytes secrete a neurotrophic factor that is important for neuronal survival (49). Furthermore, axonal growth is induced and regulated by signals from oligodendrocytes independent of myelin formation (39). Thus, it is plausible that a neurotrophic factor is deficient in oligodendrocytes that show abnormal tau accumulation.

We have shown remarkable activation of microglia at all levels of the cerebellar output pathway in PSP. Furthermore, microglial burden was associated with severity of GD in the DH. Thus, microglia in the downstream pathways may also contribute to GD. Although activation of microglia has been documented in PSP (50, 51), information on microglia in PSP is extremely limited. Microglia secrete inflammatory cytokines, free radical-related toxic molecules and as yet unidentified neurotoxic products that can produce tissue injury (52–55). For example, tumor necrosis factor (TNF), which can be found in activated microglia (56), has the potential to exert toxic effects on myelin and oligodendrocytes (57). Microglia may produce not only a direct toxic effect, but also an indirect one through astrocytes (51, 52). The demyelinated axons may be more susceptible to these toxic microglial mediators. On the other hand, we could not demonstrate a close correlation between microglial burden and either myelin loss, axonal loss, or tau burden. Thus, a plausible mechanism for microglial involvement in GD remains uncertain. Given their role as scavenger cells, microglial activation in the cerebellar output pathway might merely be secondary to fiber degeneration. Phagocytosis of myelin debris by microglia was a frequent finding in this study. Further studies regarding the pathologic roles of microglia in PSP are warranted.

Upstream Pathology

We also found that increased tau and microglial burden in the cerebellar WM correlated with severity of GD and that microglial burden in the cerebellar WM correlated with loss of GAP-43 immunoreactivity in the DN. Moreover, loss of GAP-43 immunoreactivity correlated with the severity of GD. These results suggest that pathology upstream of the DN may also be involved in GD. GD has been shown in electron microscopic studies to represent alterations of Purkinje cell axonal terminals, which contain aggregated mitochondria, synaptic vesicles, neurofilaments, lamellar bodies, and vacuoles (2, 7). GAP-43 is synthesized in the cytoplasm and transported down the axon to the regenerating or growing axon terminal (17). As such, GAP-43 is a marker for axonal terminals, in the case of the DN, most likely derived from Purkinje cells (58). We expected, but did not find GAP-43 immunolabeling of GD. In contrast, GAP-43 was decreased in GD and the severity of GD was inversely proportional to GAP-43 immunoreactivity. This might argue against the possibility that GD is a regenerative process (7, 15, 16), but rather degeneration or collapse of Purkinje cell axon terminals.

As previously discussed, if oligodendrocyte tau pathology and microgliosis in the cerebellar WM leads to damage in Purkinje cell axons, this may lead to reduction of GAP-43 at the axon terminals. The preservation of Purkinje cells in spite of possible axonal dysfunction may be reasonable given the known resistance of Purkinje

←

Fig. 8. Double-immunostaining with LN-3 (brown) and PHF-1 (purple) counterstained with LFB (blue) in controls (A, C, E, G) and PSP (B, D, F, H). A, B: ventrolateral nucleus of the thalamus (VL); C, D: red nucleus (RN); E, F: dentate hilus; G, H: cerebellar hemispheric white matter (C–F, 412×; A, B, G, H, 206×). In all the areas studied, microglia were remarkably increased both in number and volume in PSP. Loss or destruction of myelin is notable in all areas studied in PSP. Phagocytosis of myelin debris by microglia was a common finding (D, F, arrows). Tau-positive lesions were abundant in the VL and RN (B, D). Microglia and tau-positive lesions were not necessarily associated or spatially co-localized.

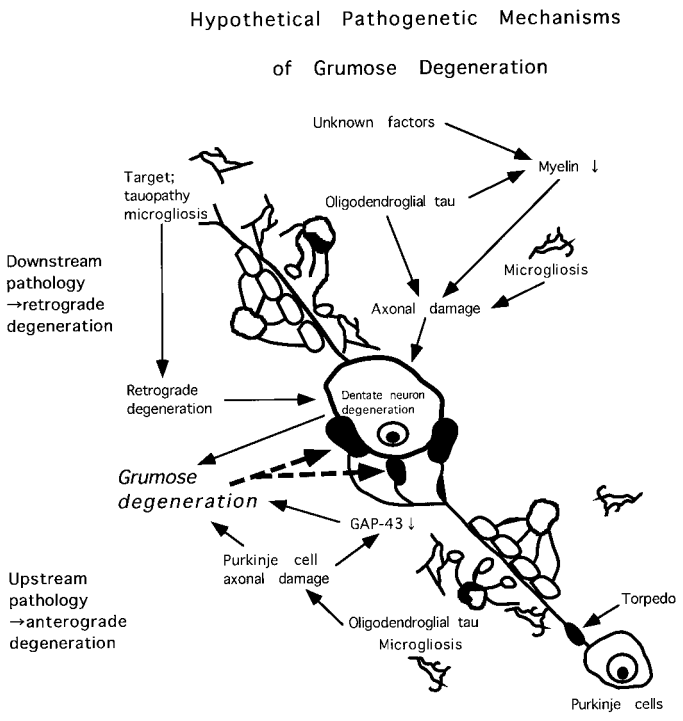

Fig. 9. Grumose degeneration (schematically shown as darkened and filled swollen distal Purkinje cell processes clustered around a dentate neuron cell body) may be due to both downstream and upstream pathology. Downstream pathology is schematically shown as degeneration and tau inclusions (darkened areas in cell bodies) in oligodendroglia, which may contribute to myelinopathy and secondary axonal degeneration. Upstream pathology includes torpedoes in Purkinje neurons (darkened and swollen segments of initial axon segments) and degeneration and tau inclusions in oligodendroglia (darkened area in cell bodies). Microgliosis is illustrated in both downstream and upstream pathways and may act to amplify the disease process.

cells to axonal injury (59). As GAP-43 is one of the molecules associated with formation of new synapses and axonal sprouting, and thus very important for neuronal growth and plasticity (17–19), its reduction in GD may contribute to the chaotic degeneration of synaptic terminals in the DN of PSP.

In addition to pathology in the cerebellar white matter, which may adversely impact on Purkinje cell axons, changes occurring closer to the Purkinje cell body should not be overlooked. In this study we found no correlation between GD and the number of Purkinje cell axonal torpedoes. This may indicate that GD is a process confined to distal portions of the Purkinje cell axon.

Conclusions

In PSP, GD occurs in the setting of neuronal and glial pathology both downstream and upstream of the DN. Figure 9 graphically summarizes possible pathogenetic mechanisms involved in GD based upon the present study. It should be emphasized that GD has been described in other disorders, such as Machado-Joseph disease or dentatorubropallidoluysian atrophy (2, 3), where the mode and degree of degeneration in upstream and downstream areas may be different from PSP. Thus, the pathogenetic mechanisms hypothesized for PSP may be different in other entities with GD. On the other hand, detailed analysis of anatomical structures using sensitive methods to detect pathology, such as immunocytochemistry for microglial changes, need to be done in a larger series of disorders with GD before this can be stated with certainty.

Despite increased knowledge of various factors that contribute to GD, the exact biological mechanism remains unknown. Determining the effects that filamentous tau inclusions may have on trophic functions of glial cells with respect to myelin and neuronal integrity are needed. In addition, it will be important to examine early cases of PSP for the light they may shed on what areas of the brain and what cell types are affected early in the disease process. In this way it may be possible to decipher primary and secondary events in complicated pathologic processes such as GD.

ACKNOWLEDGMENTS

The authors thank Virginia Phillips and Linda Rousseau for their expert technical assistance and Tien V. Le for his invaluable suggestions with image analysis. Some of the cases used in this study were donated to the Society for Progressive Supranuclear Palsy brain bank and generous donations of family members in this endeavor are greatly appreciated.

REFERENCES

1. Anzil AP. Progressive supranuclear palsy, case report with pathological findings. Acta Neuropathol 1969;14:72–76
2. Arai N. ''Grumose degeneration'' of the dentate nucleus. A light and electron microscopic study in progressive supranuclear palsy and dentatorubropallidoluysial atrophy. J Neurol Sci 1989;90: 131–45
3. Takiyama Y, Oyanagi S, Kawashima S, et al. A clinical and pathologic study of a large Japanese family with Machado-Joseph disease tightly linked to the DNA markers on chromosome 14q. Neurology 1994;44:1302–8
4. Kumada S, Hayashi M, Umitsu R, et al. Neuropathology of the dentate nucleus in developmental disorders. Acta Neuropathol 1997;94:36–41
5. Janota I. Pathological changes in the terminal parts of Purkinje cell axons in the dentate nucleus of the cerebellum. J Neurol Neurosurg Psychiatry 1973;36:596–603
6. Cruz-Sanchez FF, Rossi ML, Cardozo A, Picardo A, Tolosa E. Immunohistological study of grumose degeneration of the dentate nucleus in progressive supranuclear palsy. J Neurol Sci 1992;110: 228–31
7. Mizusawa H, Yen SH, Hirano A, Llena JF. Pathology of the dentate nucleus in progressive supranuclear palsy: A histological, immunohistochemical and ultrastructural study. Acta Neuropathol 1989;78:419–28
8. Voogd J, Feirabend HKP, Schoen JHR. Cerebellum and precerebellar nuclei. In: Paxinos G, eds. The human nervous system. San Diego: Academic Press, Inc., 1990:321–86

9. Hauw JJ, Daniel SE, Dickson D, et al. Preliminary NINDS neuropathologic criteria for Steele-Richardson-Olszewski syndrome (progressive supranuclear palsy). Neurology 1994;44:2015–19
10. Litvan I, Agid Y, Calne D, et al. Clinical research criteria for the diagnosis of progressive supranuclear palsy (Steele-Richardson-Olszewski syndrome): Report of the NINDS-SPSP international workshop. Neurology 1996;47:1–9
11. Lantos PL. The neuropathology of progressive supranuclear palsy. J Neural Transm (Suppl) 1994;42:137–52
12. Steele JC, Richardson JC, Olszewski J. Progressive supranuclear palsy. Arch Neurol 1964;10:333–59
13. Behrman S, Carroll JD, Janota I, Matthews WB. Progressive supranuclear palsy, clinico-pathological study of four cases. Brain 1969;92:663–78
14. Suyama N, Kobayashi S, Isino H, Iijima M, Imaoka K. Progressive supranuclear palsy with palatal myoclonus. Acta Neuropathol 1997;94:290–93
15. Okumura A, Oda M, Iwase S, Shiraki H. Pathomorphological and clinicopathological study of so-called grumose degeneration in the cerebellar dentate nucleus. Adv Neurol Sci (Tokyo) 1977;19: 483–92
16. Shiraki H, Okumura A, Oyanagi S. Neuropathology of ''grumose degeneration'' of the cerebellar dentate nucleus with special reference to certain neurotoxic disorders and other pathological processes. In: Roizin L, Shiraki H, Grcevic N, eds. Neurotoxicology. New York: Raven Press, 1977:43–55
17. Irwin N, Madsen JR. Molecular biology of axonal outgrowth. Pediatr Neurosurg 1997;27:113–20
18. Aigner L, Arber S, Kapfhammer JP, et al. Overexpression of the neural growth-associated protein GAP-43 induces nerve sprouting in the adult nervous system of transgenic mice. Cell 1995;83: 269–78
19. Benowitz LI, Routtenberg A. GAP-43: An intrinsic determinant of neuronal development and plasticity. Trends Neurosci 1997;20: 84–91
20. Honer WG, Kaufmann CA, Davies P. Characterization of a synaptic antigen of interest in neuropsychiatric illness. Biol Psychiatry 1992;31:147–58
21. Wolozin BL, Pruchnicki A, Dickson DW, Davies P. A neuronal antigen in the brains of Alzheimer patients. Science 1986;232: 648–50
22. Ksiezak-Reding H, Dickson DW, Davies P, Yen SH. Recognition of tau epitopes by anti-neurofilament antibodies that bind to Alzheimer neurofibrillary tangles. Proc Natl Acad Sci USA 1987;84: 3410–14
23. McGeer PL, Itagaki S, Boyes BE, McGeer EG. Reactive microglia are positive for HLA-DR in the substantia nigra of Parkinson's and Alzheimer's disease brains. Neurology 1988;38:1285–91
24. Honer WG, Hu L, Davies P. Human synaptic proteins with a heterogeneous distribution in cerebellum and visual cortex. Brain Res 1993;609:9–20
25. Greenberg SG, Davies P, Schein JD, Binder LI. Hydrofluoric acid-treated tau PHF proteins display the same biochemical properties as normal tau. J Biol Chem 1992;267:564–69
26. Kinney HC, Brody BA, Kloman AS, Gilles FH. Sequence of central nervous system myelination in human infancy. II. Patterns of myelination in autopsied infants. J Neuropathol Exp Neurol 1988;47: 217–34
27. Sternberger NH, Sternberger LA, Ulrich J. Aberrant neurofilament phosphorylation in Alzheimer disease. Proc Natl Acad Sci USA 1985;82:4274–76
28. Thomas PK, Scaravilli F, Belai A. Pathologic alterations in cell bodies of peripheral neurons in neuropathy. In: Dyck PJ, Thomas PK, eds. Peripheral neuropathy, 3rd edition. Philadelphia: Saunders, 1993:476–513
29. Barron KD, Doolin PF, Oldershaw JB. Ultrastructural observations on retrograde atrophy of lateral geniculate body. J Neuropathol Exp Neurol 1967;26:300–26
30. Feringa ER, Gilbertie WJ, Vahlsing HL. Histologic evidence for death of cortical neurons after spinal cord transection. Neurology 1984;34:1002–6
31. Ha H, Liu CN. Cell origin of the ventral spinocerebellar tract. J Comp Neurol 1968;133:185–206
32. Chung HD. Retrograde crossed cerebellar atrophy. Brain 1985;108: 881–95
33. Hanyu H, Arai H, Katsunuma H, Fujita R, Tomori C. [Crossed cerebellar atrophy following cerebrovascular lesions] (in Japanese with English abstract). Nippon Ronen Igakkai Zasshi 1991;28: 160–65
34. Matsumoto R, Nakano I, Arai N, Suda M, Oda M. Progressive supranuclear palsy with asymmetric lesions in the thalamus and cerebellum, with special reference to the unilateral predominance of many torpedoes. Acta Neuropathol 1996;92:640–44
35. Feasby TE, Hahn AF, Brown WF, Bolton CF, Gilbert JJ, Koopman WJ. Severe axonal degeneration in acute-Guillain-Barré syndrome: Evidence of two different mechanisms? J Neurol Sci 1993;116: 185–92
36. Scolding N, Franklin R. Axon loss in multiple sclerosis. Lancet 1998;352:340–41
37. Trapp BD, Peterson J, Ransohoff RM, Rudick R, Mork S, Bo L. Axonal transection in the lesions of multiple sclerosis. N Engl J Med 1998;338:278–85
38. Windebank AJ, Wood P, Bunge RP, Dyck PJ. Myelination determines the caliber of dorsal root ganglion neurons in culture. J Neurosci 1985;5:1563–69
39. Sanchez I, Hassinger L, Paskevich PA, Shine HD, Nixon RA. Oligodendroglia regulate the regional expansion of axon caliber and local accumulation of neurofilaments during development independently of myelin formation. J Neurosci 1996;16:5095–5105
40. Yin X, Crawford TO, Griffin JW, et al. Myelin-associated glycoprotein is a myelin signal that modulates the caliber of myelinated axons. J Neurosci 1998;18:1953–62
41. Fruttiger M, Montag D, Schachner M, Martini R. Crucial role for the myelin-associated glycoprotein in the maintenance of axon-myelin integrity. Eur J Neurosci 1995;7:511–15
42. Chin SSM, Goldman JE. Glial inclusions in CNS degenerative diseases. J Neuropathol Exp Neurol 1996;55:499–508
43. Papp MI, Kahn JE, Lantos PL. Glial cytoplasmic inclusions in the CNS of patients with multiple system atrophy (striatonigral degeneration, olivopontocerebellar atrophy and Shy-Drager syndrome). J Neurol Sci 1989;94:79–100
44. Matsuo A, Akiguchi I, Lee GC, McGeer EG, McGeer PL, Kimura J. Myelin degeneration in multiple system atrophy detected by unique antibodies. Am J Pathol 1998;153:735–44
45. Pakalnis A, Drake ME, Huber S, Paulson G, Phillips B. Central conduction time in progressive supranuclear palsy. Electromyogr clin Neurophysiol 1992;32:41–42
46. Abbruzzese G, Tabaton M, Morena M, Dall'Agata D, Favale E. Motor and sensory evoked potentials in progressive supranuclear palsy. Mov Disord 1991;6:49–54
47. Ikeda K, Akiyama H, Haga C, Kondo H, Arima K, Oda T. Argyrophilic thread-like structure in corticobasal degeneration and supranuclear palsy. Neurosci Lett 1994;174:157–59
48. Komori T, Shibata N, Kobayashi M, Sasaki S. Argyrophilic meshwork structures in the cerebral cortex of patients with progressive supranuclear palsy. Neuropathology 1996;16:1–5
49. Meyer-Franke A, Kaplan MR, Pfrieger FW, Barres BA. Characterization of the signaling interactions that promote the survival and growth of developing retinal ganglion cells in culture. Neuron 1995;15:805–19

50. Kida E, Barcikowska M, Niemczewska M. Immunohistochemical study of a case with progressive supranuclear palsy without ophthalmoplegia. Acta Neuropathol 1992;83:328–32
51. Komori T, Shibata N, Kobayashi M, Sasaki S, Iwata M. Inducible nitric oxide synthase (iNOS)-like immunoreactivity in argyrophilic, tau-positive astrocytes in progressive supranuclear palsy. Acta Neuropathol 1998;95:338–44
52. Dickson DW, Lee SC. Chapter 4, microglia. In: Davies RL, Robertson DM, eds. Textbook of neuropathology, third edition. Baltimore: Williams & Wilkins, 1997:165–205
53. Klegeris A, McGeer PL. Rat brain microglia and peritoneal macrophages show similar responses to respiratory burst stimulants. J Neuroimmunol 1994;53:83–90
54. Klegeris A, McGeer PL. Beta-amyloid protein enhances macrophage production of oxygen free radicals and glutamate. J Neurosci Res 1997;49:229–35
55. Giulian D, Haverkamp LJ, Yu JH, et al. Specific domains of beta-amyloid from Alzheimer plaque elicit neuron killing in human microglia. J Neurosci 1996;16:6021–37
56. Dickson DW, Lee SC, Mattiace LA, Yen SH, Brosnan C. Microglia and cytokines in neurological disease, with special reference to AIDS and Alzheimer's disease. GLIA 1993;7:75–83
57. Selmaj KW, Raine CS. Tumor necrosis factor mediates myelin and oligodendrocyte damage in vitro. Ann Neurol 1988;23:339–46
58. Buffo A, Holtmaat AJ, Savio T, et al. Targeted overexpression of the neurite growth-associated protein B-50/GAP-43 in cerebellar Purkinje cells induces sprouting after axotomy but not axon regeneration into growth-permissive transplants. J Neurosci 1997;17:8778–91
59. Dusart I, Sotelo C. Lack of Purkinje cell loss in adult rat cerebellum following protracted axotomy: Degenerative changes and regenerative attempts of the severed axons. J Comp Neurol 1994;347:211–32

Received September 30, 1999
Revision received February 28, 2000
Accepted March 1, 2000